Eur. Phys. J. D **11**, 481–489 (2000)

THE EUROPEAN PHYSICAL JOURNAL D

EDP Sciences

Auto-solitary solutions in a generalized model of gas discharge contraction

G.R. Sonnemann[1,a] and V.E. Semenov[2,b]

[1] Leibniz-Institute of Atmospheric Physics at the University of Rostock, 18225 Kühlungsborn, Germany
[2] Institute of Applied Physics, Russian Academy of Sciences, 603600 Nizhny Novgorod, Russia

Received 26 July 1999 and Received in final form 5 February 2000

Abstract. Stable auto-solitary solutions were found on the basis of three-dimensional numerical simulations within the simplest model under global constraint. The model involves a diffusion equation with a nonlinear source term containing both local and non-local nonlinearity. The source term was chosen so as to describe qualitatively the most fundamental peculiarities of discharge physics, namely local nonlinear increase in heating and ionization rate and non-local attenuation of electric field strength with plasma density growth. The properties of the autosolitons created by the model have been investigated employing the different parameters as control parameter. Therefore the results of calculations can be used to construct a process of plasma contraction in gas discharge.

PACS. 52.35.Sb Solitons; BGK modes – 52.50.-b Plasma production and heating – 52.35.Py Plasma macroinstabilities (hydromagnetic, e.g., kink, fire-hose, mirror, ballooning, tearing, trapped-particles, flute, Rayleigh-Taylor, etc.)

1 Introduction

The investigation of localized domains in dissipative systems has been marked by increasing interest over the past two decades. There is a broad bibliography on this subject. In the monograph written by Kerner and Osipov [1] these phenomena have been named autosolitons. Such spotted patterns are special dissipative structures. They occur in very different scientific disciplines such as physics, medicine, technology, ecology, etc. (as also quotations in Falcke [2] and Aranson *et al.* [3], Gorshkov *et al.* [4], Deissler and Oron [5], and Yakhno [6]). The theoretical study of autosolitons is typically based on a set of coupled diffusion type equations with nonlinear sources (Vasillev *et al.* [7]). However, as was found by Sonnemann [8,9] such structures also appear within a special immunological system under global constraints. The later means that a local evolution of a considered field depends on its global (integral) quantities. In other words, the model involves a set of integro-differential equations.

In this paper we investigate stable autosolitons occurring in a simplified system under global constraint which presents a generalized description of plasma contraction phenomenon in gas discharge. It should be noted that many localized structures of different types were revealed in gas discharge. Some of them are caused mainly by local effects while non-local interaction is very important for others. Kerner and Osipov [1] studied the autosolitions of the first type and showed that the stable structures are possible only in the case when at least two diffusion processes are coupled due to nonlinear sources. Surprisingly, as will be shown and discussed in the following sections, the global constraint provides stability of the autosoliton if even only one of the diffusion equations is considered.

2 General description of the physical model

The contraction phenomenon was first observed in a positive column of glow discharge. In experiments (Golubovskii *et al.* [10,11]) plasma filled the whole cross-section of the discharge tube for a sufficiently small value of the discharge current, while for a higher current the plasma is concentrated near the tube axis if the gas pressure was not too small. The phenomenon was explained by increase of ionization and gas heating rate caused by their mutual influence. The simplest mathematical model of this thermal contraction is based on the heat-transfer equation with a nonlinear source (Velikhov *et al.* [12]):

$$c\frac{\partial T}{\partial t} = \nabla(\lambda\nabla T) + \sigma(T, E)E^2 \qquad (1)$$

where T is the gas temperature, t the time, c and λ are the specific heat capacity and the thermal conductivity of gas, respectively, E stands for the electric field strength which is homogeneous in the tube, and σ represents the

[a] e-mail: sonnemann@iap-kborn.de
[b] e-mail: sss@appl.sci-nnov.ru

electric conductivity of ionized gas increasing with growth of T or/and E. The electric field strength depends on the voltage across a resistance in the external circuit, *i.e.* it is controlled by the total electric current J in the discharge tube:

$$EL = E_0 L - RJ \tag{2}$$

where E_0 expresses the electric field strength in the absence of current, R stands for the load resistance in the external circuit, L describes the length of the discharge tube. The total current is determined by the integral of the current density over the cross-section of the tube. Hence, it is given by

$$J = \int \sigma E \mathrm{d}s = E \int \sigma \mathrm{d}s. \tag{3}$$

Equations (2, 3) give us the integral dependence of E on plasma conductivity:

$$E = \frac{E_0}{1 + (R/L) \int \sigma \mathrm{d}s} \cdot \tag{4}$$

From mathematical point of view the set of equations (1, 4) represents a simple case of nonlinear diffusion equation under global constraint which suppresses a nonlinear growth of the source.

The contraction phenomenon was also observed in a discharge sustained inside of a quasi optic resonator fed by microwave radiation (Kapitsa [13], Vikharev *et al.* [14,15]). In these experiments the electric field intensity was not homogeneous in space due to the formation of electromagnetic standing wave structure. Therefore the plasma did not fill the whole volume of the resonator. Even for a small input value of microwave power (that corresponded to the non-contracted regime of discharge), the plasma was localized in the vicinity of the highest maximum of the standing wave structure. In other words, plasma occupied a region whose characteristic size corresponds to about the length of the standing wave, *i.e.* much smaller compared to the resonator size. Nevertheless, if the gas pressure exceeded a definite threshold value, an increase of the input of microwave power led to a considerable decrease in plasma size which becomes much less compared to the wavelength. In contrast to glow discharge where the contraction is associated with the occurrence of 2D structures, a real 3D localization of plasma is observed in microwave discharge.

In principle, in microwave discharge the process of gas heating itself does not differ from that in glow discharge and equation (1) can also be used for its description. The only difference in this case is the dependence of σ on E and T. Specifically, the increase of σ with growth of T is characterized by saturation at a definite value of T depending on gas pressure and field frequency (Kim and Fraiman [16]). Due to the mismatch between resonator and feeding microwave generator, there is also a specific dependence of the electric field intensity on the integral of σ over the volume of the resonator (Vikharev *et al.* [17]), *i.e.* on the total number of electrons in the plasma since the conductivity is proportional to the plasma density. (This is a consequence of the fact that the plasma is only weakly ionized in gas discharge.) This dependence is more complicated compared to (4). However, a sufficiently large value of $\oint \sigma \mathrm{d}\tau$ also leads to a decrease in the field intensity. Hence, it is possible to discuss the thermal contraction in microwave discharge exploiting a mathematical model similar to (1–4).

It should be mentioned that alternative physical mechanisms of the microwave discharge contraction are also considered in the literature. An influence of the excitation of gas molecules and the transition from the free electron diffusion to the ambipolar diffusion were discussed (Golubovskii and Lyagushenko [10], and Egley and Engel [18]) and local perturbation of the electric field amplitude were considered (Gildenburg and Kim [19]). The role of negative ions was taken into account by Novata and Kando [20] and Vikharev *et al.* [14,15]. However, in each case the mathematical model includes one or more diffusion type equations with nonlinear sources depending on electric field intensity which is determined by the integral value of unknown functions. Within such a model the parameters of the stationary solution were calculated for different conditions and found to be in reasonable agreement with experimental results. At the same time a detailed analysis of the stability of the stationary localized structures has not been completed. Consequently, there is no proof of the existence of the autosolitons themselves thus far. Moreover, it is not known how many combined nonlinear equations of diffusion type under global constraints are necessary to provide auto-solitary solutions.

In this paper it is shown by numerical simulations that stable autosolitons are possible even for only one diffusion equation. In order to get a more general model of contraction the equation (1) was modified:

$$\frac{\partial U}{\partial t} = \nabla (D \nabla U) + A[U] \Phi(U) - \nu U \tag{5}$$

where U represents a generalized characteristic of discharge (given by such quantities as gas temperature, plasma density, concentration of excited molecules, etc.), D stands for the effective diffusivity (diffusion coefficient) and ν is the effective loss frequency (which equals zero for the thermal mechanism of the contraction but differs from zero for the alternative mechanisms). The function $\Phi(U)$ describes the nonlinear source (heating, ionization, excitation, etc.). The functional $A[U]$ simulates the dependence of the electric field intensity on the total amount of electrons in discharge plasma. It can be expressed as a decreasing function of the integral of U over the volume (if U corresponds to plasma density):

$$A = A_0 (1 + \oint U \mathrm{d}\tau)^{-\beta}, \tag{6}$$

or as a decreasing function of the integral of $\Phi(U)$ over the volume (if U corresponds to the gas temperature):

$$A = A_0 (1 + \oint \Phi(U) \mathrm{d}\tau)^{-\beta}. \tag{7}$$

Here the coefficient A_0 describes a power of an external energy source (microwave generator), and the exponent β depends on the considered physical mechanism of the contraction. Typically, the local source $\Phi(U)$ increases rapidly with growth of its argument U but this increase has a tendency to saturation with large values of U. In this paper such a dependence was simulated by a function

$$\Phi(U) = \frac{U^\alpha}{1+U^\alpha} \tag{8}$$

with a constant exponent α. The proposed model can only be considered a first step to describe the localized structures of microwave discharge. It is certainly too rough to claim any quantitative comparison with experiments. Specifically, this model cannot describe a transition from quasi-homogeneous regime of discharge to its contracting regime when the parameters (gas pressure and microwave power) are changed. Nevertheless, there is hope that the model could be useful in understanding the main qualitative peculiarities of the contraction phenomenon: the existence of stable localized structures and conditions of their formation, namely, sufficiently high input power (high value of A_0) and sufficiently high gas pressure (low value of diffusivity D).

3 Description of the numerical model

We use a similar three-dimensional model as described in detail in Sonnemann [9]. It is a Cartesian co-ordinate gridpoint system consisting of $51\times51\times51$ gridpoints. The flux through the boundary is chosen to be zero. This is justified if the size of an autosoliton is sufficiently small compared with the size of the gridpoint domain. The size of an autosoliton can be defined, for instance, by the half-value diameter. On the other hand, in order to minimize numerical errors, the autosoliton should be large compared with the gridpoint distance. Cartesian co-ordinates have the advantage that multiple autosolitons can be better modelled than by spherical co-ordinates. However, in this paper we present only results of a single autosoliton. We use arbitrary units here called arbitrary units of space (AUS), arbitrary units of time (AUT) and with respect to the quantity U of equation (5) arbitrary units of U (AUU). The basic equation can be written as

$$\frac{\partial U}{\partial t} = \frac{AU^\alpha}{(1+U^\alpha)} - \nu U + D\Delta U \tag{9}$$

with A corresponding to (6).

The exponent α has been fixed at $\alpha = 5$ for the most numerical calculations. The prefactor A_0 has also been fixed at $A_0 = 1$. The diffusion coefficient D, the so-named loss frequency ν and the parameter β have been chosen as control parameters.

It should be mentioned that the use of $A_0 = 1$ is not connected with a loss of generality. Division of equation (9) by A_0 leads to a normalized time $t^* = A_0 t$ and changed loss frequency $\nu^* = \nu/A_0$ and diffusion coefficient $D^* = D/A_0$. Therefore, we can investigate the influence of A_0 on the autosolitons when considering different values of D and ν provided that the ratio D/ν is kept constant.

$\Delta = \partial^2/\partial\mathbf{r}^2$ represents the Laplacian with $\mathbf{r}$ – space vector. $\oint U\mathrm{d}\tau$ stands for the total integral of U over the whole space. We call this value also the bulk of U. Equations (9, 6) describe a system under global constraint.

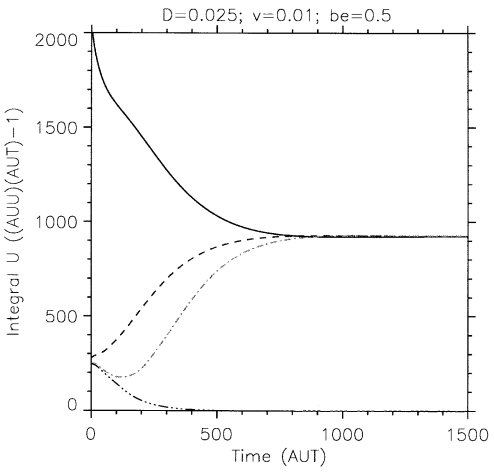

Fig. 1. Dependence of the time behaviour of integral U on the initial conditions. Parameter: $D = 0.025(AUS)^2(AUT)^{-1}$, $\nu = 0.01(AUT)^{-1}$, $\beta = 0.5$ and $\alpha = 5$.

4 Results

4.1 Dependence on the initial conditions

$U \equiv 0$ is a stable solution. Any small perturbation p vanishes in the course of time because of $p^\alpha \ll \nu p$ for $\alpha > 1$. We call $U \equiv 0$ the trivial homogeneous solution. The most important quantity is the integral of U over the whole space. $\oint U\mathrm{d}\tau \equiv 0$ is valid for the trivial solution, otherwise (excluding negative solutions as physically unreasonable) it has a positive value. We start our computation in any case with the trivial solution $U \equiv 0$ superimposed by one (or more) differently extended parcel(s) of perturbation(s) for which $U > 0$ is valid and is located in the single case around the center (or also distributed in another way).

Figure 1 shows the time behaviour of the integral U for 4 different initial conditions for fixed system parameters. It was $D = 0.025(AUS)^2(AUT)^{-1}$, $\beta = 0.5$ and $\nu = 0.01(AUT)^{-1}$. The computation starts with a perturbation within the central grid points 23 to 29 for all co-ordinates with $U \equiv 6$, $U \equiv 0.8$, $U \equiv 0.72$ and $U \equiv 0.71(AUU)$ beginning with the uppermost curve to the lowest one. Evidently, there is a critical initial perturbation for U between $U = 0.71$ and $U = 0.72(AUU)$ for which the final state changes. In the first case the solution runs into a non-trivial value, in the second case the solution approaches the trivial distribution $U \equiv 0$. In the non-trivial case the upper three curves run independently of the initial values into the same final state.

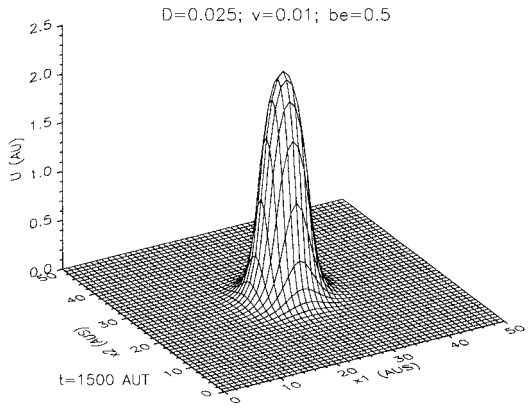

Fig. 2. Distribution of U in the X_1-X_2-plane. The same parameters as in Figure 1 are used.

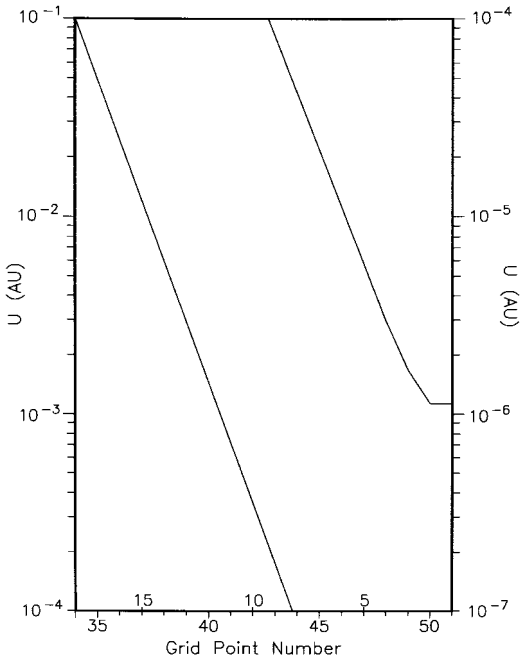

Fig. 3. Behaviour of U within the atmosphere of the autosoliton according to Figure 2 in logarithmic scale showing the exponentially decreasing amount of U. The right scale is valid for the right curve.

The third curve near the critical threshold for the initial values shows a tendency to approach the trivial solution in the first stage but finally it reaches the non-trivial solution.

The critical amounts of the initial values depend on the size of the parcels. It is important that there are critical initial perturbations and that the final state in the non-trivial case does not depend on the shape and size of the initial perturbation. This is also valid for extremely shaped initial perturbations.

Figure 2 displays the distribution of U in the $X_1 - X_2$-plane in a surface plot. There is a stable localized domain which is also called a spotted pattern or autosoliton. This autosoliton is a spherical object with a core domain and an atmosphere of strong decreasing values of U with increasing distance from the core region. The highest values occur around the center.

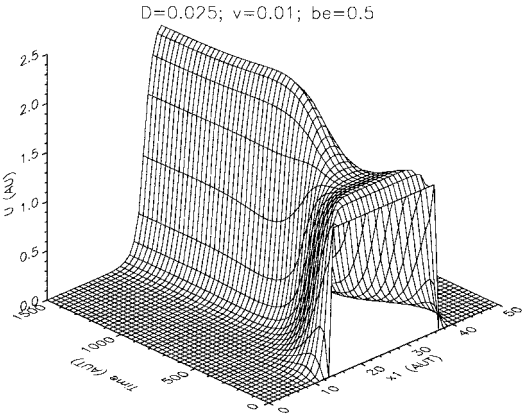

Fig. 4. Time behaviour of U across the X_1-axis starting with a stick-shaped initial perturbation approaching a spherical autosoliton also in this extreme case. The same parameters as in Figure 1 are used.

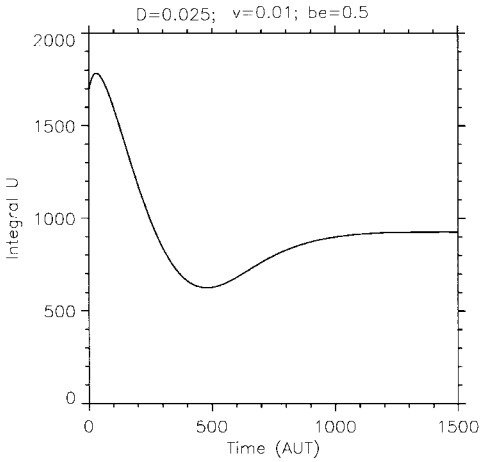

Fig. 5. Time behaviour of Integral U for the example depicted in Figure 4. The final value tallys with that of Figure 1 of the non-trivial cases.

Away from the center the quantity U decreases nearly linearly within the core region. This figure also demonstrates that the flux out of the gridpoint box would be nearly zero even without the special boundary conditions.

Figure 3 shows the behaviour of U within the atmosphere of the autosoliton. U decreases exponentially there. The few gridpoints near the boundary are influenced by the boundary conditions. Although U possesses only very small values the atmosphere of an autosoliton has a very important meaning in case of multiple autosolitons as we will discuss elsewhere. These findings confirm results derived from computations of autosolitons on the basis of a more complex system describing immunological processes (Sonnemann [8,9]).

In a surface plot Figure 4 depicts the time behaviour of U across the X_1-axis using a stick-shaped initial condition. The initial conditions are $U = 1.5(AUU)$ for the gridpoints 15 to 37 of the X_1-co-ordinate and for 23 to 29

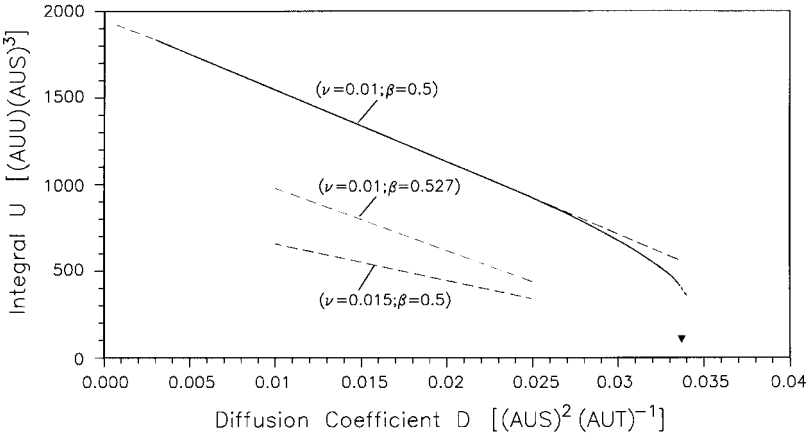

Fig. 6. Dependence of integral U on the diffusion coefficient for different sets of the parameters ν and β.

of the other ones again. The system approaches the same spherical autosoliton even in this extreme case.

Figure 5 displays the course of the integral U which illustrates that, although beginning with high values of the integral, the amount decreases below the final value during the shrinking phase. The autosoliton approaches a spherical shape independent of the initial perturbation like here using the stick-shaped initial conditions.

The velocity to approach this final state depends, above all, on the diffusion coefficient. The characteristic diffusion time τ_{D} can be written as

$$\tau_{\mathrm{D}} = \frac{H_U^2}{D} \tag{10}$$

where H_U is the space-scale of U defined by the absolute amount of the inverse logarithmic derivative with respect to the space:

$$\frac{1}{H_U} = \left| \frac{1}{U} \frac{\partial U}{\partial \mathbf{r}} \right| . \tag{11}$$

This means for very small diffusion coefficients the system needs a very long time to reach an approximately steady state. It is interesting to note that the scale of U is constant within the atmosphere. Because of the discrete gridpoint structure numerical uncertainties arise in case of small diffusion coefficients so that we excluded the value region $D < 0.003(AUS)^2(AUT)^{-1}$. Evidently, the shape of the initial condition is preserved for a long time and can even be numerically locked by the discrete gridpoints.

4.2 Dependence of the auto-solitary solution on the system parameters

From a mathematical point of view (9) possesses the potential to have a nontrivial stable stationary homogeneous solution under certain conditions. For the homogeneous solution $\partial U/\partial t = 0$ and $D\Delta U = 0$ is valid.

However, this solution does not apply to the quasi-homogeneous regime of gas discharge and it would be necessary to use another model for this case. Consequently, we do not consider the homogeneous solution here.

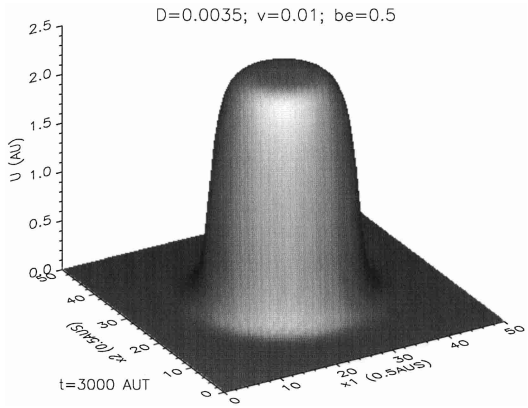

Fig. 7. Distribution of U over the X_1-X_2-plane for a small diffusion coefficient of $D = 0.0035(AUS)^2(AUT)^{-1}$ demonstrating the occurrence of a central plateau of the distribution within the autosoliton.

We now investigate how the autosolitons change if we use the system parameter D, ν and β as control parameter. The auto-solitary solution does not depend on the size of the grid-point box but the numerical accuracy will improve if the spatial resolution becomes higher. In order to produce the following figures some hundred single computations have been carried out.

Figure 6 shows the dependence on the diffusion coefficient D for certain arbitrary values of ν and β. As mentioned earlier, the range of very small diffusion coefficients has been excluded. We can first recognize that there is a linear dependence of the integral U, that is to say bulk of the autosoliton, on the diffusion coefficient for a certain range of values of D. The higher the diffusion coefficient is, the smaller the bulk is. Secondly, there is a boundary of the existence of autosolitons for large diffusion coefficients. The exact border of the critical diffusion coefficient cannot be determined precisely because the basin of attraction for the auto-solitary solution shrinks to zero near the critical diffusion coefficient. The boundary value in Figure 6 has been determined by the step-by-step reduction of D after reaching an auto-solitary solution and amounts about to $D = 0.03(AUS)^2(AUT)^{-1}$.

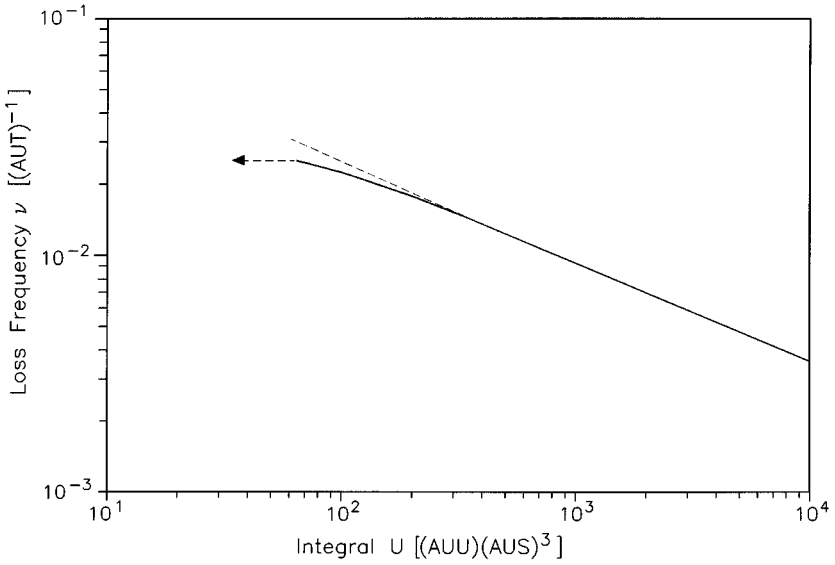

Fig. 8. Dependence of integral U on the loss frequency ν in double logarithmic scale. The same parameters as in Figure 1 are used with the exception of ν.

Thirdly, close to the critical diffusion coefficient the linear dependence of integral U on D loses its validity. The integral decreases more strongly than linear. This behaviour is imaginable. Figure 7 exhibits the distribution of U over the X_1-X_2-plane for $D = 0.0035(AUS)^2(AUT)^{-1}$. The spatial resolution was reduced by a factor of 0.5. Comparing this figure with Figure 2 one can see that the distribution of U within the autosoliton shows more of an internal plateau for $D = 0.0035(AUS)^2(AUT)^{-1}$ than for larger D-values. For larger amounts of D the distribution becomes sharper and the peak value diminishes.

From Figure 6 one can derive

$$\oint U \mathrm{d}\tau = aD + b \tag{12}$$

for the range of validity of the linear dependence. As the calculations show the parameters a and b are functions of the system parameters ν and β, $a = a(\nu, \beta)$ and $b = b(\nu, \beta)$. For the concrete values of Figure 6, $\nu = 0.01(AUT)^{-1}$ and $\beta = 0.5$, follows $a \approx -42750(AUU)(AUS)(AUT)$ and $b \approx 1990(AUU)(AUS)^3$. Both the lower dashed curves in Figure 6 exhibit the linear behaviour for changed parameters within a limited range of D-values. However, the linear expression (12) is only an approximation. The integral approaches most probably a finite value when D goes to zero. This value can be estimated if using the approach given in the Appendix. The extrapolation of the linear expression (12), when D goes to zero, and the estimated bulk of the autosoliton, when using the analytical equation (A.5) given in the Appendix, are in reasonable agreement.

Figure 8 shows the dependence of $\oint U \mathrm{d}\tau$ on the loss frequency ν in double logarithmic scale. As to be expected, the amount of the integral increases strongly with decreasing loss frequency. For sufficiently small ν-values the dependence is close to a power law as predicted by an analytical approach (see Appendix). However, there is the smallest autosoliton (the boundary autosoliton) again. Close to the boundary autosoliton the simple functional coherence gets lost as the rising difference to the dashed line indicates. The size of the autosoliton increases strongly with decreasing ν, whereas the maximum value of U does not considerably change. This is consistent with analytical predictions, too.

The dependence of the bulk value on the parameter β is still more sensitive than for the previous parameters. As Figure 9 illustrates, the bulk value of the autosoliton increases strongly with decreasing β when ν is small. For a high β-value a boundary autosoliton occurs again. With exception of the vicinity of the boundary autosoliton, the numerical calculated dependence of $\oint U \mathrm{d}\tau$ on β is not far from analytical estimations (see Appendix). With the change of the system parameters the shape of the autosolitons also changes. When enlarging, for instance, the loss frequency the most striking feature is a shrinking of the diameter. The smallest bulk of the autosoliton seems to be unconfined, but only in a certain parameter set where one parameter acts as a control parameter and the remainder are fixed. Figure 10 shows the shape of an autosoliton for a relatively small diffusion coefficient of $0.01(AUS)^2(AUT)^{-1}$ but larger loss frequency of $\nu = 0.1(AUT)^{-1}$. The bulk value amounts only to $9(AUU)(AUS)^3$.

The last parameter not considered thus far is the exponent α. It was fixed in the previous calculations to $\alpha = 5$. We now investigate what happens if α varies at fixed values $D = 0.01(AUS)^2(AUT)^{-1}$, $\beta = 0.5$ and $\nu = 0.01(AUT)^{-1}$. Figure 11 depicts the results. For large values of α the increase of the bulk of the autosoliton is only very small for further increasing α and it seemingly approaches a final value. A minimum occurs near $\alpha = 3$. For smaller values of α the bulk values increase strongly.

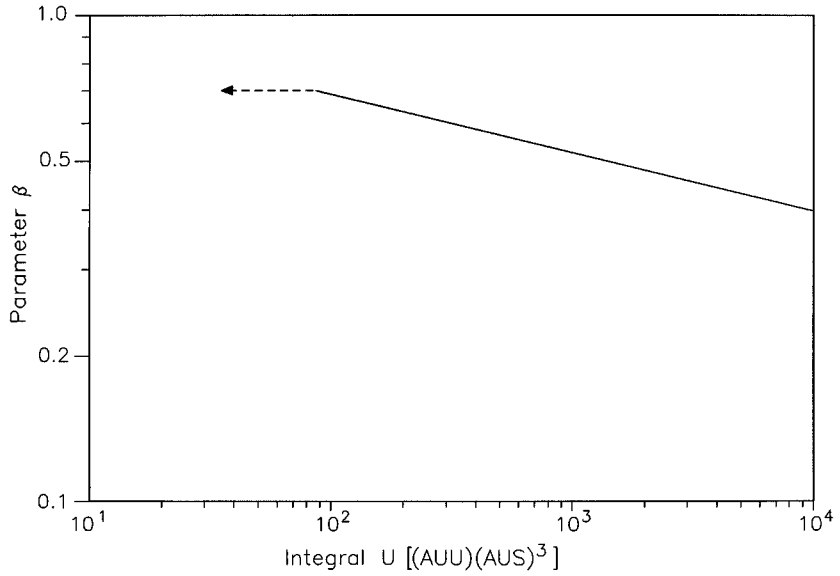

Fig. 9. Dependence of integral U on the parameter β in double logarithmic scale. The same parameters as in Figure 1 are used with the exception of β.

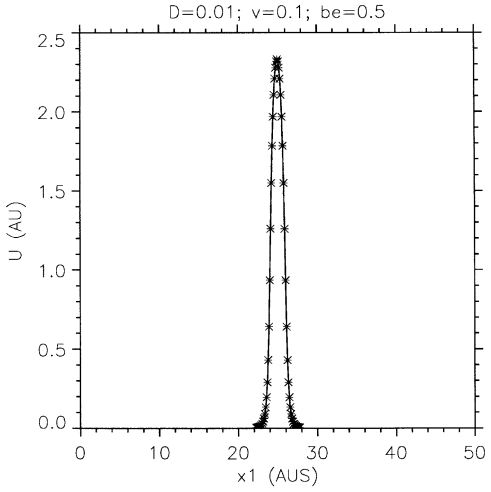

Fig. 10. Shape of an autosoliton across the X_1-axis for a relatively small diffusion coefficient of $0.01(AUS)^2(AUT)^{-1}$ but larger loss frequency $\nu = 0.1(AUT)^{-1}$ showing a needlelike form. The parameter β and α as in Figure 1 are used.

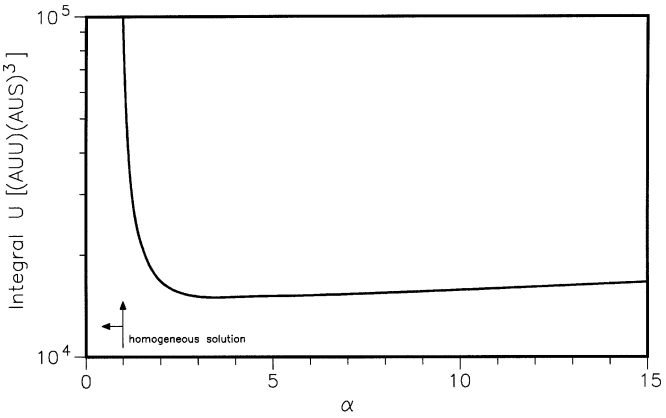

Fig. 11. Dependence of the integral U on the parameter α. The remaining parameters as in Figure 1 are used.

Simultaneously the diameter of the autosoliton grows but the peak value of U decreases noticeably. There seems to be a boundary value of α for which an autosoliton can arise. For $\alpha \leq 1$ there is apparently only the homogeneous solution but in the vicinity of $\alpha = 1$ an autosoliton-like feature lasts very long. Figures 12 and 13 display this behaviour for $\alpha = 1$ after very long time steps of $3000(AUT)$ and $6000(AUT)$. Note that the scale of the $X_1 - X_2$-plane has been enlarged and the scale for U has been drastically reduced.

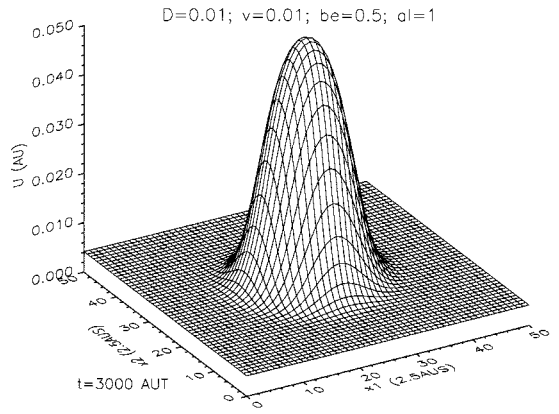

Fig. 12. A very long lasting autosolitonlike pattern for $a = 1$ after $3000(AUT)$. The final state is the non-trivial homogeneous solution. The remaining parameters as in Figure 1 are used but $D = 0.01(AUS)^2(AUT)^{-1}$.

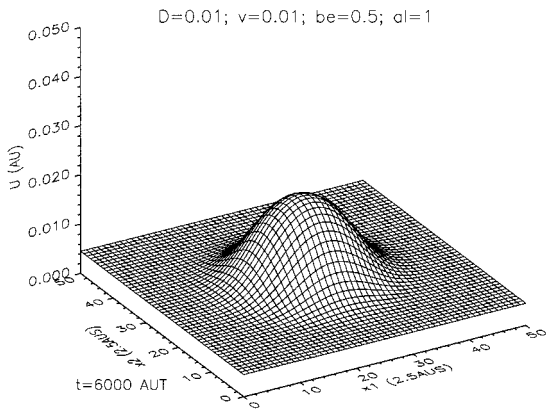

Fig. 13. A very long lasting autosolitonlike pattern for $a = 1$ after $6000(AUT)$. The final state is the non-trivial homogeneous solution. The remaining parameters as in Figure 1 are used but $D = 0.01(AUS)^2(AUT)^{-1}$.

5 Discussion

The numerical investigation of the relatively simple equation (9) being an equation under global constraint and having only one variable U surprisingly yields results which are very similar to those obtained by employing a more complex system as summarized in Sonnemann [9]. Based on an immunological question a five-component reaction-diffusion system under global constraints had been introduced which could also create auto-solitary solutions. The time behaviour of this system and its solution showed common properties. This concerns such features as a stable trivial solution (healthy), a critical infection in order to become ill, the possibility of getting a non-trivial homogeneous solution and, as said before, the development of autosolitons.

Using only a two-component system consisting of an activator and an inhibitor no auto-solitary solution occurred but only a burning out within a decreasing domain. This behaviour is not so surprising because in contrast to equation (9) of this paper the two-component system did not have any limiting factor. The limiting factor of (9) which prevents an unlimited rise of U is given by $(1 + U^{\alpha})^{-1}$ corresponding to (8). Nothing in nature can grow unlimitedly, there are always restricting factors. One of them in immunology or also ecology is the limited food supply in reality which confines an unlimited increase of every species. Such limiting terms also have to include in the two component model.

A characteristic property of autosolitons of this kind is that they are structureless and consequently without internal dynamics. A single autosoliton is fixed at a certain place. A movement of a single autosoliton requires an external U-field having a certain gradient. An autosoliton does not have a fixed border, it is actually unlimited but one can define a size of such a localized domain using, for example, the half-value diameter or any other definition. Another important finding is that there is a boundary autosoliton – a smallest or weakest autosoliton – for each set of system parameters.

As initially mentioned autosolitons are a phenomenon sometimes observed in connection with plasma contraction of gas discharge. In experiments the contraction was observed for high pressure (*i.e.* low value of the ratio D/ν) and for sufficiently high power (*i.e.* low value of D provided the ratio D/ν is kept constant). Our calculations give evidence that the simplified model qualitatively describes this behaviour.

Appendix A

Below we represent comments on a qualitative analysis of the stationary localized solution of the time-independent equation (5):

$$\nabla(D\nabla U) + A(U)\Phi(U) - \nu U = 0 \qquad \text{(A.1)}$$

where

$$A = (1 + \oint U \mathrm{d}\tau)^{-\beta}. \qquad \text{(A.2)}$$

If a characteristic radius R_{C} of an autosoliton is much larger than the characteristic diffusion length $L_{\mathrm{D}} = \sqrt{D/\nu}$ the autosoliton should have a flat top with $U \approx U_{\mathrm{m}}$ where U_{m} is the maximum root of the equation:

$$A\Phi(U) - \nu U = 0. \qquad \text{(A.3)}$$

The bulk of the autosoliton can be estimated as $(4\pi/3)R_{\mathrm{C}}^3 U_{\mathrm{m}}$.

Figure 7 showed an example of an autosoliton marked by a flat top.

Simultaneously the thickness of the boundary layer is of the order of $L_{\mathrm{D}} \ll R_{\mathrm{C}}$. Therefore, the structure of this layer can be considered by an 1D analogy of equation (A.1). An analysis brings us to the conclusion that the boundary layer (a jump from $U \approx U_{\mathrm{m}}$ to $U \approx 0$) is possible if and only if the following relation is valid:

$$\int_0^{U_{\mathrm{m}}} [A\Phi(U) - \nu U] \, \mathrm{d}U = 0. \qquad \text{(A.4)}$$

A solution of equation (A.3, A.4) gives the definite values of the ratio (ν/A) and U_{m} which are independent of the parameters D, ν and β. Respectively, equation (A.2) can be used to determine the bulk $\oint U \mathrm{d}\tau$ of an autosoliton and its radius R_{C}. Specifically for $\alpha = 5$, one can obtain from (A.3, A.4) that approximately it is then

$$U_{\mathrm{m}} \approx 2.053 \qquad \text{and} \qquad \left(\frac{\nu}{A}\right) \approx 0.474. \qquad \text{(A.5)}$$

Therefore, in the considered case, equation (A.2) results in the following estimate for the bulk of the autosoliton

$$\oint U \mathrm{d}\tau = A^{-1/\beta} - 1 \cong (0.474/\nu)^{1/\beta} - 1 \cong \frac{8\pi}{3} R_{\mathrm{C}}^3. \qquad \text{(A.6)}$$

As mentioned, the derived results (Eqs. (A.5, A.6)) should be corrected when $L_{\mathrm{D}} \ll R_{\mathrm{C}}$ is valid. It is interesting to note that the boundary autosolitons found in Section 4.2 are closely connected with the violation of the inequality. In particular, in all cases, the ratio $(R_{\mathrm{C}}/L_{\mathrm{D}})$ is estimated to be about 3.4 to 3.5 for the boundary values of the parameters ν, D and β.

References

1. B.S. Kerner, V.V. Osipov, *Autosolitons*, edited by A. van der Merwe (Kluwer Academic Publishers, Dortrech/Boston/London, 1994).
2. M. Falke, *Pattern formation in reaction-diffusion systems under global constraints* (Wissenschaft und Technik Verlag, Berlin, 1995, *in German*).
3. I.S. Aranson, K.A. Gorshkov, A.S. Lomov, M.I. Rabinovich, Physica D **43**, 435 (1990).
4. K.A. Gorshkov, A.S. Lomov, M.I. Rabinovich, Nonlinearity **5**, 1343 (1992).
5. R.J. Deissler, A. Oron, Phys. Rev. Lett. **68**, 2948 (1992).
6. V.G. Yakhno, Optim. Mem. Neutr. Net. **4**, 141 (1995).
7. V.A. Vasillev, Yu.M. Romanovskii, D.S. Chernavskii, V.G. Yakhno, *Autowave processes in kinetic system, Spatial and Temporal Self-organization in Physics, Chemistry, Biology, and Medicine*, edited by W. Ebeling, Ch. Weißmantel, (VEB Deutscher Verlag der Wissenschaften, Berlin, 1987).
8. G. Sonnemann, Thesis B, Acad. Sciences of the GDR, 1984 (in *German*).
9. G. Sonnemann, Progr. Theor. Phys. **99**, 931 (1998).
10. Yu.B. Golubovskii, R.I. Lyagushenko, Sov. Phys.-Tech. Phys. (USA) **22**, 1073 (1977) [Zh. Tekh. Fiz. (USSR) **47**, 1852 (1977)].
11. Yu.B. Golubovskii, A.K. Zinchenko, Yu.M. Kagan, Sov. Phys.-Tech. Phys. (USA) **22**, 851 (1977) [Zh. Tekh. Fiz. (USSR) **47**, 1478 (1977)].
12. E.P. Velikhov, A.S. Kovalev, A.T. Rakhimov, *Physical Phenomena in Gas Discharge Plasma* (Nauka, Moscou, 1987, *in Russian*).
13. P.L. Kapitsa, Zh. Eksp. Teor. Fiz. **57**, 1801 (1969) (in *Russian*).
14. A.L. Vikharev *et al.*, Sov. Phys. Dokl. (USA) **32**, 581 (1987) [Dokl. Akad. Nauk SSSR (USSR) **295**, 358 (1987)].
15. A.L. Vikharev, O.A. Ivanov, O.Yu. Kuznetsov, A.N. Stepanov, Sov. J. Plasma Phys. (USA) **13**, 648 (1987) [Sov. J.: Fiz. Plasmy (USSR) **13**, 1124 (1987)].
16. A.V. Kim, G.M. Fraiman, Sov. J. Fiz. Plazmy **9**, 613 (1983); on the nonlinear stage of ionization-thermal instability in high frequency das discharge at high pressure (in *Russian*); also published in Sov. J. Plasma Phys. (USA) **9**, 358 (1983).
17. A.L. Vikharev, O.A. Ivanov, L.S. Ivanova, O.Yu. Kuznetsov, A.N. Stepanov, Sov. Zhu. Tekh. Fiz. **59**, 40 (1989) (in *Russian*).
18. P.D. Egley, A. Engel, *Proc. 10th Int. Conf. on Phenomena in Ionized Gases*, Oxford, 1971, p. 1116.
19. V.B. Gildenburg, A.V. Kim, Sov. Phys. JETP **47**, 72 (1978).
20. K. Novata, M. Kando, J. Appl. Phys. **50**, 3956 (1979).